Cold-induced serum short-chain fatty acids act as markers of brown adipose tissue metabolism in humans

Milena Monfort-Pires[1*], Mueez U-Din[1,2], Vanessa de Mello[3], Teemu Saari[1], Juho Raiko[4], Edla Kerminen[1], Johan Rajander[5], Kati Hanhineva[6], Tobias Fromme[7], Rikard Landberg[8], Martin Klingenspor[9], Kirsi A. Virtanen[1,2*]

[1] Turku PET Centre, University of Turku, 20540, Turku, Finland

[2]Turku PET Centre, Turku University Hospital, Turku, Finland

[3]Institute of Public Health and Clinical Nutrition, School of Medicine, University of Eastern Finland, 70211, Kuopio, Finland.

[4]Turku PET Centre, Turku University Hospital, Turku, Finland; Kanta-Häme Central Hospital, Hämeenlinna, Finland

[5]Turku PET Centre, Accelerator Laboratory, Åbo Akademi University, Turku, Finland

[6]Department of Public Health and Clinical Nutrition, University of Eastern Finland, Kuopio, Finland; Department of Life Technologies, Food Chemistry and Food Development Unit, University of Turku, Turku, Finland; Department of Biology and Biological Engineering, Division of Food and Nutrition Science, Chalmers University of Technology, Gothenburg, Sweden.

[7]Chair for Molecular Nutritional Medicine, TUM School of Life Sciences, Research Department of Molecular Life Sciences, Technical University of Munich, Freising, Germany. EKFZ-Else Kröner Fresenius Center for Nutritional Medicine, Technical University of Munich, Munich, Germany.

[8]Division of Food and Nutrition Science, Department of Life Sciences, Chalmers University of Technology, Gothenburg, Sweden.

[9]Chair for Molecular Nutritional Medicine, Technical University of Munich, Freising, Germany; EKFZ - Else Kröner Fresenius Center for Nutritional Medicine, Technical University of Munich, Freising, Germany; ZIEL - Institute for Food & Health, Technical University of Munich, Freising, Germany.

* Corresponding author

Milena Monfort-Pires: orcid.org/0000-0002-1652-8083

mmopir@utu.fi

Kirsi A. Virtanen

kianvi@utu.fi

Keywords: Short-chain fatty acids, brown adipose tissue, cold exposure, PET/CT scan

Declaration of interests

The authors declare no competing interests.

Abstract

Background: Short-chain fatty acids (SCFAs) produced from dietary fibre fermentation can regulate adipose tissue metabolism through signalling pathways involving G-protein-coupled receptors and histone deacetylase inhibition. While preclinical studies suggest they enhance thermogenesis, their role in human brown adipose tissue (BAT) under different thermal conditions remains unclear. **Objective:** This study explores the associations between circulating SCFAs and human BAT metabolism at room temperature and after cold exposure. **Methods:** This cross-sectional study included data from 71 adults (20–55 years, BMI 19–44 kg/m²). Dynamic [^{15}O]O_2, [^{15}O]H_2O, [^{18}F]FDG, and [^{18}F]FTHA PET/CT scans were used to assess BAT metabolism. Serum SCFAs were quantified using LC-MS, and gene expression in biopsy-excised BAT samples (n=14) was analysed. Participants were stratified into low- and high-BAT groups based on [^{18}F]FDG or [^{18}F]FTHA uptakes. **Results:** Cold-induced acetate and propionate were positively associated with key in vivo BAT metabolism indicators, namely non-esterified fatty acids (NEFA) uptake and oxygen consumption. Only in the high-BAT group were circulating SCFAs maintained after cold exposure. BAT transcriptome revealed that genes involved in SCFA metabolism (such as conversion to acetyl-CoA) correlated with thermogenic and lipid metabolism genes exclusively in the high-BAT group, suggesting a distinct molecular link between SCFA pathways and BAT function. **Conclusion:** Circulating SCFAs are linked with BAT oxidative metabolism and NEFA uptake during cold exposure. The observed correlations between SCFA catabolic genes and thermogenic markers suggest that metabolically active BAT may selectively engage SCFA-related pathways, pointing to a potential mechanistic role of SCFAs in supporting BAT function in humans.

Introduction

It has long been known that fibre intake is associated with favourable metabolic outcomes (1,2), though only recently have some of these effects been linked to the actions of short-chain fatty acids (SCFAs) (2,3). Acetate, propionate, and butyrate are produced in the colon by various bacterial families through the fermentation of dietary fibre, including resistant starch and, to a lesser extent, proteins (3–5). Although less than 10% of these SCFAs enter systemic circulation, they can still act as substrates or signalling molecules regulating diverse metabolic processes (3,5).

The beneficial effects of SCFA are shown to be primarily mediated by SCFAs functioning as ligands for G-protein coupled receptors (GPCRs), particularly GPR43 and GPR41 (3,6,7). Among them, there is evidence that butyrate can enhance whole-body insulin sensitivity by promoting glucose uptake in muscle and adipose tissue and suppressing hepatic glucose production, thereby supporting glycemic control (8). Acetate, conversely, serves as a substrate for cytosolic acetyl-CoA synthesis, contributing to lipogenesis and other acetyl-CoA–dependent processes critical for adipose tissue metabolism and function (9). Emerging evidence points to the fact that butyrate and acetate influence the secretion of gut-derived hormones such as peptide YY (PYY) and glucagon-like peptide-1 (GLP-1) by activating GPCRs (3,6,10,11). These SCFAs also act as signalling molecules, exerting systemic effects across various tissues (12). Notably, acetate has been linked to reduced food intake and suppressed orexin neuronal activity in ob/ob mice (13). Beyond metabolic regulation, SCFAs are linked to anti-inflammatory effects, as they can inhibit the production of pro-inflammatory cytokines and reduce systemic inflammation (6,14). These immunomodulatory actions are thought to be mediated in part by

SCFA-induced inhibition of histone deacetylases (HDACs), particularly via GPR41 and GPR43 signalling—a mechanism considered central to the regulatory role of SCFAs (6,11,15).

Unlike white adipose tissue (WAT), which primarily serves as an energy reservoir, brown adipose tissue (BAT) dissipates energy as heat, positioning it as a promising target for cardiometabolic disease treatments (16–19). While the interaction between SCFAs and BAT function in humans remains underexplored, SCFAs are known to modulate adipose tissue metabolism by regulating lipolysis and lipogenesis (2,5,20). In vitro studies indicate that butyrate and propionate can induce WAT browning, enhance mitochondrial function, and boost energy expenditure via activation of AMP-activated protein kinase (AMPK) and peroxisome proliferator-activated receptor gamma (PPAR-γ) pathways (21–23). The thermogenic effects of SCFAs also occur via the sympathetic nervous system, which leads to enhanced WAT browning and non-shivering thermogenesis (5,8). Some studies show that SCFAs can also inhibit adipogenesis by suppressing lipogenic enzymes and promoting lipolysis, thereby preventing excessive fat accumulation (14,24). Additionally, experimental data indicate that acetate and butyrate enhance BAT activity by upregulating thermogenic genes such as UCP1 (5,25), alongside improvements in overall energy metabolism by increasing fatty acid oxidation in BAT (15). Indeed, in rodents, acetate injections have been shown to reduce lipid accumulation in BAT while increasing the expression of lipolytic genes (25).

SCFAs exert beneficial metabolic effects through mechanisms involving the activation of GPCRs in different tissues (3,6,10). Rodent studies further highlight the crucial role of SCFAs in regulating WAT and BAT metabolism (5,8,25). However, the interaction between SCFAs and brown adipose tissue (BAT), particularly under cold exposure and thermoneutrality conditions, remains poorly understood in humans. To address this gap, the present study investigated the associations between circulating SCFAs—acetate, propionate, and butyrate—and BAT metabolism in adult humans at room temperature and after acute cold exposure. Even though

there are no standard thresholds to classify individuals as low or high-BAT, we stratified our sample into low and high-BAT to better understand how having more active BAT affects circulating SCFAs and gene expression profiles. Lastly, we explored the correlations between genes involved in SCFAs signalling pathways (such as components of the SCFA utilisation pathway, encompassing SCFA transport, mitochondrial conversion, and downstream metabolic regulation in BAT) and those regulating thermogenesis, lipolysis, and lipogenesis in BAT.

Material and Methods

Study design and participants

This cross-sectional data included seventy-one subjects from studies conducted at the Turku PET Centre between 2009 and 2018 (26–29). Imaging and biological data are derived from previous studies investigating human BAT metabolism. These cohorts' inclusion and exclusion criteria have been previously published (27,29)

Twenty-two males and 49 females were included in this study. The group had an age range of 20–55 years and a body mass index (BMI) range of 18.9-43.7 kg/m^2. All participants were clinically assessed before recruitment into the respective studies, and those presenting an overall healthy metabolic profile with no diabetes and/or cardiovascular diseases were included. A metabolic health profile was assessed and determined based on available medical records, a 2-h oral glucose tolerance test (OGTT), an electrocardiography (ECG) assessment, circulating lipids, and hepatic enzymes profile. All recruited study subjects provided written informed consent for volunteering in the clinical research studies. The Hospital District of Southwest Finland Ethics Committee gave their favourable opinion for the study protocols, and the studies were conducted according to the principles of the Declaration of Helsinki (27–29).

All PET/CT imaging and blood samples were collected after an overnight fast. The subjects were instructed to refrain from consuming alcoholic and caffeinated beverages for 12 hours

before the metabolic assessments. Additionally, participants were advised to avoid strenuous physical activity for 24 hours before the study.

Biochemical data

As previously described, fasting blood samples were used for biochemical analyses to measure plasma total cholesterol, HDL, and triglycerides photometrically (ModularP800, Roche Diagnostics). LDL cholesterol was calculated using the Friedewald equation. Whole-body insulin sensitivity was assessed using hyperinsulinemic-euglycemic clamp (M-value) (27–29).

PET/CT imaging

The scanning protocol was conducted during cold exposure using a personalised cooling protocol for both studies: For study one, on the cold exposure day, the subjects spent two hours wearing light clothing in a room with an ambient temperature of 17°C before the PET imaging. During the imaging (ambient temperature of 23°C), cold exposure was induced by placing one foot intermittently (5 min in/5 min out) in water at a temperature of 8°C on average (26). For study 2, the cooling was 2 hours before the PET scan using cooling blankets, 6°C water, and then increased water temperature when shivering was observed (objective observation by a researcher). During the imaging, the cooling protocol was maintained (27).

The PET imaging of the supraclavicular region was carried out while the subject was in a supine position. For study one, the glucose uptake rate in the target tissues (BAT, WAT) was measured using the [^{18}F]FDG radiotracer. For study 2, the non-esterified fatty acids (NEFA) uptake rate (µmol/100 g/min) was analysed using the [^{18}F]FTHA radiotracer. Tissue perfusion at room temperature and after cold exposure was assessed using [^{15}O]H_2O (mL/100g/min), whereas metabolic rate of oxygen (MRO_2) was analysed using [^{15}O]O_2 (mL/100g/min) (27). As previously described, BAT radiodensity (measured with Hounsfield Units – HU) was analysed using CT

images (30). All PET scans were performed using a dynamic acquisition protocol as previously described (27,30).

PET/CT imaging analysis

PET/CT imaging data were analysed using Carimas software (version 2.8, Turku PET Centre, Finland) and Vinci 2.54.0 software (Max-Planck Institute, Cologne, Germany). Glucose and NEFA uptake were analysed using the Patlak-Gjedde plot (31,32). Subjects were categorised as high-BAT or low-BAT based on substrate uptake rates (^{18}F-FDG and/or ^{18}F-FTHA) in supraclavicular BAT depot. Specifically, individuals were classified as high-BAT if they had a glucose uptake rate of ≥3.0 µmol/100 g/min or a non-esterified fatty acid (NEFA) uptake rate of ≥0.7 µmol/100 g/min. The threshold for the glucose uptake rate of 3.0 µmol/100 g/min is based on a 3-fold increase during cold exposure compared to resting, room temperature measurements (1.0 µmol/100 g/min) (29). The threshold aligns with a standardised uptake value (SUV) of 1.5 g/mL (30), the recommended SUV for BAT detection according to the BARCIST 1.0 criteria (33). The NEFA uptake rate of 0.7 µmol/100 g/min is equivalent to the energy content of glucose following complete oxidation.

White and brown adipose tissue biopsies and RNA sequencing

The biopsy of supraclavicular adipose tissue for WAT and BAT was taken from 14 volunteers (30). BAT depots in this region were identified using available imaging data, such as MRI or cold-exposed [^{18}F]FDG PET and [^{18}F]FTHA PET/CT scans. A subcutaneous adipose tissue sample was collected from the same incision site as a WAT reference. The procedure was conducted at room temperature (~22°C) under local anaesthesia with lidocaine-epinephrine and performed by a plastic surgeon. Immediately after extraction, tissue samples were frozen in liquid nitrogen to preserve their integrity.

Deep-frozen adipose tissues (30–120 mg) were homogenised in TRIsure, and RNA was extracted, purified using spin columns, and eluted in water. RNA concentration was measured (Nanodrop ND-1000), diluted (25–500 ng/mL), denatured (70°C, 2 min), and assessed for integrity (Bioanalyzer 2100). Coding RNA was enriched (TruSeq RNA Access) to compensate for degradation, and sequencing was performed (HiSeq 2500, Illumina). Gene expression levels were quantified as RPKM (27,28).

SCFA quantification

Targeted quantification of short-chain fatty acids (SCFAs: acetate, propionate, butyrate) and succinate was performed using an LC-MS method developed and validated at Chalmers University of Technology (34). Standards were sourced from Honeywell (acetate), Alfa Aesar (propionate), Sigma Aldrich (butyrate), and Acros (succinate). Derivatisation reagents (3-NPH, EDC-6, quinic acid, pyridine, methanol, water) were from Sigma Aldrich; acetonitrile was from Fisher Scientific. A $^{13}C_6$-3NPH-HCl internal standard, synthesised by IsoSciences Inc., was used for quantification. Stock solutions of standards were prepared in 75% methanol at specified concentrations and diluted 1:10 in 10% methanol. Calibration curves ranged 3.2 µM–0.63 nM (acetate), 3.2 µM–0.31 nM (propionate), and 0.8 µM–0.16 nM (butyrate, succinate). Samples were analysed in batches, and each batch included five blanks and three triplicate quality control samples (two long-term pooled plasma samples; one cohort-specific plasma sample).

Statistical analysis

All statistical analyses were performed using IBM SPSS Statistics 28.0.1. Figures were drawn using GraphPad Prism and Python. Data are presented as mean and standard deviation or standard error of the mean. The normality of data was checked using the Kolmogorov-Smirnov test. Because most variables were not normally distributed, the Spearman correlation coefficients were used for correlation analyses, and a false discovery rate (FDR) test for multiple

comparisons was applied (correlation heat maps). For the correlations between circulating SCFA and imaging parameters, the variables were log-transformed, and the Pearson coefficient was employed. Low-BAT and high-BAT correlation coefficients were compared using the Fisher r-to-z test. An independent t-test (or Mann-Whitney U) was also used to compare low-BAT and high-BAT groups. For paired analysis (WAT versus BAT gene expression in the same group of individuals), a paired-sample t-test (or Wilcoxon) was employed.

Results

Characteristics of the sample

The main characteristics of the sample are presented in Table 1. As previously mentioned, the cutoff used to categorise volunteers as low and high-BAT aligns with an SUV of 1.5 g/mL, and its application allowed for the detection of significant group differences, supporting its utility in this context. Therefore, Table 1 shows the volunteers' baseline characteristics according to low- or high-BAT groups. Predictably, the high-BAT group consisted of younger, leaner individuals with better metabolic profiles, such as lower concentrations of total and LDL-cholesterol and triglycerides (TG), higher HDL levels, and higher insulin sensitivity, as assessed by the M-value ($p<0.05$ for all). Only body fat percentage was similar between the groups. It is important to emphasise that this data has been previously shown by our group (30).

No differences between the two groups were detected regarding circulating SCFAs at room temperature (RT). However, we observed higher concentrations of cold-induced (CI) propionate ($p=0.02$) and a trend of higher concentrations of CI-acetate in the high-BAT group when compared to low-BAT ($p=0.06$), suggesting that these SCFAs could be modulated by acute cold exposure. Differences in BAT-imaging data between groups were expected because we used

CI-NEFA uptake and glucose uptake rate (GUR) to stratify the groups. Still, no differences were detected for GUR and oxygen metabolic rate (MRO_2) at RT and CI-MRO_2 (p=0.078), most likely due to the small sample size for these measurements.

Associations between imaging data, circulating cardiometabolic markers, and SCFA

Next, we sought to understand how SCFAs were associated with BAT function. Therefore, we analysed the correlations between RT and CI-SCFAs with BAT variables (GUR, NEFA uptake rate, and MRO_2 in BAT) under RT and cold-induced conditions (Figure 1 and Supplementary Table 1)(35). Interestingly, CI-acetate was directly correlated with CI-NEFA uptake (r = 0.62; p<0.01), whereas CI-propionic acid was associated with the CI-MRO_2 (r=0.62; p<0.01). Moreover, CI-acetate correlated with RT and CI circulating free fatty acids (CI-FFA) (p<0.01, Supplementary Table 1) (35). In contrast, RT-acetate was associated with CI-FFA, BAT radiodensity, and CI-BAT NEFA uptake (Supplementary Table 1) (35). Nevertheless, after FDR correction, only the associations between FFAs and acetate remained significant (Supplementary Table 1) (35). In addition, RT and CI-butyrate were associated with BAT radiodensity. In contrast, CI-acetate concentrations were inversely correlated with clinical markers such as body weight, BMI, and waist and hip circumference. At the same time, RT acetate was associated with M-value (p<0.01, not significant after FDR correction). RT and CI-butyrate were also inversely correlated with waist circumference, while CI-butyrate was also associated with M-value (Supplementary Table 1) (35).

Changes in acetate, butyrate and propionate after cold exposure

Because we observed correlations between CI-SCFA and imaging data and cold stress could affect SCFA levels (36), (18), we investigated how acetate, propionate, and butyrate levels were modulated during acute cold exposure. We observed that propionate and butyrate levels were lower after cold exposure than RT (Figures 1H and 1I), but no significant changes were detected in acetate concentrations (Figure 1G).

Differences between low-BAT and high-BAT groups

To better understand how changes in SCFA were affected by having a higher or lower BAT metabolism, we investigated whether cold-induced changes in SCFA were different when comparing low-BAT and high-BAT volunteers. Even though acetate concentrations were similar between low and high-BAT groups (Figure 2A), in the high-BAT group, propionate and butyrate levels were maintained after two hours of cold exposure (Figures 2B, 2C). We only observed reductions in serum propionate (Figure 2B) and butyrate (Figure 2C) after cold exposure in the low-BAT group. Moreover, the low-BAT group showed lower propionate concentrations after cold exposure (Figure 2B).

Differences between the low-BAT and high-BAT groups were also observed when analysing the correlations between SCFA and clinical variables (Figure 2D-2G and Supplementary Table 2) (35). Positive associations between BAT NEFA uptake and CI-acetate were only detected in the high-BAT group (rho=0.781; $p<0.01$) (Figure 2G), whereas CI-propionate was associated with the MRO_2 in BAT (rho = 0.857; $p<0.05$) only in the low-BAT group (Figure 2F). On the other hand, RT propionate and butyrate were inversely associated with cold-induced NEFA uptake in the low-BAT but not in the high-BAT group (Figures 2D, 2E). A significant association between CI acetate and CI-FFAs was only found for the latter group (Figure 2G). Concerning clinical variables, RT-butyrate correlated with M-value (rho = 0.703; $p<0.01$) and CI-butyrate with HDL only in the high-BAT group. Conversely, RT-acetate was inversely correlated with body weight, while CI-propionate was associated with LDL and total cholesterol in the low-BAT group (Figure 2D-2G and Supplementary Table 2) (35).

Gene expression associations between SCFA metabolic pathways with β-oxidation, de novo lipogenesis (DNL) and thermogenic markers

Because SCFAs have been shown to act as substrates for BAT function via *de novo* lipogenesis (DNL), converted into acetyl-CoA for the TCA cycle during acute cold exposure, and influence

HDACs, we sought to investigate how thermogenic genes were correlated to SCFA metabolic pathway (i.e. enzymes promoting de novo lipogenesis from SCFA and catabolic pathways) gene expression in BAT samples. When we analysed the entire sample (Supplementary Figure 1) (35), we observed strong associations between *ACSS1* with *SIRT3* and *ACSS3* with *HADH, FASN*, and *CEBPA*. Other genes associated with the SCFA catabolic pathways (*PCCA, PCCB, MUT, HADH, HADHA, HADHB, and ECSH1*) were correlated both to β-oxidation genes (such as *AKT2, CPT2,* and *PRKAKA*) and to the genes in the DNL/FA synthesis pathways (*ACACA, ACLY, ELOVL6*). In addition, these genes showed strong positive associations with thermogenic markers (*UCP-1, CIDEA, DIO2*, and *PPPARGC1A*, $p<0.05$ after FDR correction, Supplementary Figure 1) (35). Remarkably, when we analyzed the association of those genes with DNL/FA synthesis, *ACLY, ACACA, ELOVL6, FASN, MLXIPL*, and *SCD* were correlated with *ACSS2* and *ACSS3*, but *ACSS1* was inversely associated with *SREBF1* and *MLXIPL*, suggesting a different role of the two enzymes in BAT.

Gene expression associations in low-BAT and high-BAT groups – browning/thermogenic markers and β-oxidation

We observed discrepancies between the groups when we investigated how these genes differentially correlated in low-BAT and high-BAT individuals (Figure 3A, 3B), as highlighted on the split-tile heat map (Figure 3C). The two groups differed in their associations between *SIRT1, SIRT3, ACSS1*, and *ACSS2* with SCFA catabolic pathway genes and thermogenic/browning genes (Figures 3A, 3B, and 3C). Only in the high-BAT group, positive associations between β-oxidation genes and genes from the SCFA catabolic pathways were detected (Figure 3B). In the low-BAT group, *PCCA, PCCB* and *MUT*, for example, were not associated with β-oxidation genes, which could suggest different SCFA handling. Moreover, positive associations were observed between *ACSS1* and *SIRT3* in high-BAT volunteers with thermogenic/browning markers (such as *UCP1, PRDM16, DIO2, CIDEA,* and *PPARGC1A).* After FDR correction,

some associations between *SIRT3* and *ACSS1* with these markers remained significant. In the low-BAT group, only *SIRT1* was associated with thermogenic markers. Moreover, in the high-BAT group, *SIRT3* was associated with *PCCB, ECSH1, HADH, and HADHA*, all of which were also linked to *CIDEA*. Other genes, such as *HADHA*, *HADHB,* and *ECSH1,* correlated with *UCP1* and/or *TMEM26* in the high-BAT group but not in the low-BAT group. In contrast, in the low-BAT group, *SIRT3* and *ACSS1* were negatively associated with browning/thermogenic genes (*UCP-1, PRDM16, DIO2,* and *CEBPA*). Using the Fisher r-to-z test, we found that correlations of *SIRT1* and *SIRT3* with thermogenic markers (*UCP1*, *DIO2*, *PRDM16*) differed significantly between high-BAT and low-BAT individuals. In high-BAT, associations between SIRT3 were predominantly positive. In contrast, they were weak or negative in low-BAT, suggesting distinct regulatory interactions between mitochondrial/SCFA pathways and thermogenic gene expression across groups (Supplementary Figure 2) (35). The opposite was detected for SIRT1 and thermogenic genes (positive associations in the low-BAT group versus negative associations in the high-BAT group).

Gene expression associations in low-BAT and high-BAT groups – DNL and fatty acid synthesis

Regarding the associations of SCFA catabolic genes and DNL/FA synthesis genes, the *ACSS2* gene was directly associated with DNL genes in both groups. However, only in the high-BAT group was *ACSS1* inversely correlated with *MLXIPL*. In addition, in the low-BAT group, the *ACSS1* gene was negatively correlated with *AKT2, CPT2,* and *MUT* genes (Supplementary Figure 3) (35). Contrary to the findings from the high-BAT group, positive associations between *ECHS1* with DNL and FA synthesis genes were observed in the low-BAT group, which could suggest that these SCFAs are more easily used for DNL in BAT of volunteers with higher BAT metabolism (high-BAT group).

Comparisons between WAT and BAT gene expression

We compared the expression of thermogenic, DNL, and SCFA pathway genes in BAT and WAT according to low- and high-BAT groups. The expressions of *PCCB* (Figure 3I) and *MUT* (Figure 3J) were shown to be higher in BAT than in WAT for both groups, whereas only in the high-BAT group did we detect higher expressions of *SIRT3* (Figure 3D) and *ACSS2* (Figure 3F) and a trend of higher expression of *ACSS1* (Figure 3E), *PCCA* (Figure 3H) compared to WAT. The comparisons between the expression of genes related to SCFA metabolism, β-oxidation, and DNL in BAT versus WAT in the whole sample are depicted in Supplementary Table 3 (35). When comparing low-BAT and high-BAT groups, only *ACSS3* in WAT was significantly higher in the high-BAT group ($p = 0.029$, data not shown), whereas *SIRT1* reached borderline significance (6.6 ± 1.1 in the low-BAT group versus 7.7 ± 0.9 in the high-BAT group, $p = 0.053$, data not shown). Even though it would be expected to have higher *ACSS1* and *ACCS2* expression in BAT of high-BAT individuals, the difference between groups was not significant ($p=0.16$, data not shown). Moreover, when comparing groups, no differences were detected for FFAR2 in WAT or BAT.

Lastly, Figure 4 depicts the proposed mechanisms by which circulating SCFA may function as markers of proper BAT function, especially concerning the uptake of fatty acids during cold exposure.

Discussion

Compelling evidence highlights the role of microbiota-derived metabolites in energy balance and adipose tissue function. Yet, research on the crosstalk between circulating SCFAs and BAT function in humans is limited. Our study aimed to explore the relationship between circulating SCFAs and BAT metabolism in adults. Cold-induced circulating acetate was associated with CI-NEFA uptake in BAT, while CI-propionate correlated with CI-BAT metabolic rate of oxygen. These results support the idea that circulating SCFAs may be valuable markers for proper BAT function. Supporting these findings, individuals in the high-BAT group had higher CI, but not RT,

SCFA levels. In BAT samples from this group, thermogenic genes like *UCP1, CIDEA*, and *PRDM16* correlated with genes involved in SCFA catabolism. Additionally, propionate-related genes (*PCCA, PCCB,* and *MUT*) were linked to β-oxidation markers, reinforcing the potential of SCFAs to indicate BAT function and facilitate FA uptake.

Several rodent studies have demonstrated SCFAs' role in adipose tissue by modulating lipolysis, lipogenesis, and thermogenesis (3,6,10,15). SCFAs serve as lipid synthesis substrates and signalling molecules that regulate adipose metabolism (6,24,37). Acetate and butyrate are readily converted into acetyl-CoA, a precursor for fatty acid and cholesterol synthesis (3), fuel for BAT and WAT under nutrient deprivation (38,39), or HDAC inhibitors affecting gene transcription (14,38,40). Still, acetate's direct effects in brown adipocytes remain contradictory (41,42). Our study showed associations between CI-acetate, circulating FFA, and CI-NEFA uptake in BAT, suggesting that acetate could be a marker of FFA uptake in BAT. Notably, this correlation was present only in individuals in the high-BAT group. No associations were seen between CI-SCFAs and CI-glucose uptake, which aligns with the understanding that BAT relies primarily on triglyceride-derived fatty acids over glucose during its activation, with SCFAs supporting this function either as energy sources or HDAC inhibitors (6,12,24,37,43). Moreover, BAT can use intracellular and extracellular lipids during cold exposure (44).

The metabolic relevance of SCFAs has also been linked to their contribution to the acetyl-CoA pool (9,38). Current evidence suggests that acetate and acetyl-CoA levels may function as metabolic sensors, connecting nutrient availability to stress responses and gene regulation (38,39). Elevated intracellular acetyl-CoA modulates histone acetylation and thus metabolic gene expression (24,38,39). While butyrate more strongly influences histone acetylation (24,45), we observed no correlation between circulating butyrate and BAT function. This may result from rapid butyrate conversion to acetyl-CoA or its use in histone acetylation during thermogenesis

(38,39). Contrary to this idea, one *in vitro* study reported that acetate inhibited thermogenic machinery in brown adipocytes, reducing mitochondrial uncoupling and fatty acid oxidation (42).

Interestingly, we also detected a strong correlation between CI-propionate and the CI-MRO_2 in BAT, observed only in the low-BAT group after stratifying the sample. *In vitro* evidence suggests that propionate activates the sympathetic nervous system, increasing heart rate, thermogenesis, and energy expenditure (46), and induces WAT browning (24,46). The absence of a similar correlation in the high-BAT group may reflect distinct mechanisms of BAT fuel utilisation and activation across groups. Although somewhat paradoxical, the correlation between CI-propionate and MRO2 in the low-BAT group might indicate increased sympathetic activity or muscle shivering, potentially explaining the observed serum propionate reductions after cold exposure. In contrast, individuals with high BAT activity may possess more efficient metabolic machinery to utilise SCFAs, whether as oxidative fuel, substrates for de novo lipogenesis, or regulators of gene transcription via histone acetylation (24,25,38,39).

Stratification of the sample also revealed distinct CI-SCFA patterns: while SCFA levels remained stable after cold in the high-BAT group, propionate and butyrate concentrations decreased in the low-BAT group. Since SCFAs can act as nutrient sensors, the stable levels in high-BAT individuals may reflect enhanced regulation of SCFA production or utilisation (possibly hepatic) to sustain thermogenesis (25,38). Cold exposure activates gut-brain communication via transient receptor potential (TRP) channels, stimulating norepinephrine release and BAT thermogenesis, while promoting WAT browning (47). In the low-BAT group, the SCFA reduction may suggest preferential use of SCFAs as readily absorbed and metabolised oxidative substrates for thermogenesis. Yet, the specific mechanisms remain uncertain. Indeed, cold-induced SCFA alterations are not well defined in humans (36,48). This means that, during cold exposure, high-BAT individuals maintain stable levels of circulating acetate and propionate—associated with BAT fatty acid uptake —while low-BAT individuals show a drop in these SCFAs,

suggesting that SCFA stability supports efficient thermogenesis and substrate handling under cold stress. However, because the effects of cold on SCFA production are controversial and not well explored in humans (36,48), intervention studies are necessary to confirm this hypothesis. A 10-day cold challenge study in mice reported impaired gut microbiota and diminished SCFA levels (36), though other studies have shown variable responses depending on exposure duration and intensity (36,48,49).

Remarkably, the absence of gut microbiota reduces rodent thermogenic capacity—a defect reversed by butyrate supplementation (48). Elevated circulating butyrate may confer a metabolic advantage by boosting mitochondrial activity and fatty acid oxidation in BAT, as shown in mice (6). Both butyrate and acetate also promote WAT browning by upregulating genes such as *UCP1, PRDM16*, and *PGC-1α,* leading to browning (15,21,23). Additionally, SCFAs—particularly acetate and butyrate—act as potent HDAC inhibitors, enhancing histone acetylation and transcription of genes involved in cell differentiation, metabolism, and anti-inflammatory pathways (15,24). In adipose tissue, HDAC3 inhibition has been linked, for example, to increased expression of PPARγ targets, improving insulin sensitivity (24). Nevertheless, the cell- and gene-specific pathways of SCFA-mediated HDAC inhibition remain only partially understood.

We also observed positive associations between serum RT and CI-acetate and propionate with the insulin sensitivity marker (M-value) and HDL cholesterol, alongside inverse correlations between RT-acetate and body weight, BMI, and waist circumference. These findings support previous associations between higher circulating SCFAs and improved lipid and glucose metabolism (2,11,50,51). SCFAs play an essential role in glucose regulation by acting on GPCRs, especially FFAR2 (GPR43), which is expressed in enteroendocrine cells and pancreatic islets (2). FFAR2 activation stimulates GLP-1 release, enhancing insulin secretion and suppressing glucagon, improving postprandial glucose control (6,24). SCFAs also regulate

energy metabolism through AMPK signalling (6,21,22), promoting mitochondrial biogenesis and glucose uptake via PGC-1α, particularly in muscle and adipose tissue (6). Unexpectedly, we detected no differences in FFAR2 expression between low- and high-BAT groups. Interestingly, most SCFA-clinical parameter associations were detected only in the high-BAT group, emphasising the relevance of elevated circulating SCFA. We hypothesise that acetate may be converted into acetyl-CoA for DNL, with newly synthesised fatty acids possibly activating UCP1 instead of being stored as triglycerides. Indeed, our transcriptome results linking the SCFAs catabolic pathway and thermogenic genes in BAT samples add significant insights to this narrative.

In high-BAT individuals, ACSS1 positively correlated with SIRT3, PGC1-α, and UCP1, and SIRT3 with all β-oxidation genes, indicating robust thermogenic capacity under cold exposure. SCFA, mainly acetate, is converted to acetyl-CoA by ACSS1, supporting energy homeostasis and mitochondrial function during fasting or ketogenic states (38,52). This means ACSS1 provides an alternative route for generating acetyl-CoA from SCFAs, mainly when nutrient availability is limited or during thermogenic events (38,52), and may influence epigenetic regulation via SIRT3-mediated deacetylation (53,54). Mice lacking ACSS1 develop hypothermia during fasting or under low-carbohydrate diets, while wild-type mice increase ACSS1 expression under similar conditions (38,55). Experimental data support the hypothesis that cold exposure and caloric restriction activate SIRT3 expression in white and brown adipose tissues (53), and SIRT3 knockout mice exhibit impaired lipid metabolism (56). Thus, in our samples, SIRT3 and ACSS1 seem to support the metabolic needs of BAT, ensuring that energy can be produced efficiently, even when substrate availability is scarce (53,57), like using SCFA during cold exposure.

We also found correlations between CIDEA and TMEM26 with SCFA-pathway catabolic genes in the high-BAT group, especially those in propionate metabolism. CIDEA was associated with

PCCA, PCCB, and MUT, which are involved in propionate catabolism. CIDEA regulates lipid droplet dynamics, controlling fatty acid availability for β-oxidation (58,59), and supports energy balance during cold or fasting (58,59). By controlling lipid droplet formation and turnover, CIDEA modulates the substrates accessible to β-oxidation enzymes (58,59). This regulation is essential for maintaining the energy balance within BAT, particularly during periods of increased energy demand, such as cold exposure or fasting (58,59). On the other hand, by deacetylating key enzymes involved in β-oxidation, SIRT3 directly enhances their metabolic efficiency, counterbalancing the lipid storage function of CIDEA (54,56,57,60). The interconnected roles of CIDEA, SIRT3, and ACSS1 in our high-BAT volunteers suggest a finely tuned regulatory network within BAT that balances energy storage and expenditure, maintaining metabolic flexibility required for effective thermogenesis, and allowing BAT to respond dynamically to physiological. Conversely, the low-BAT group showed negative associations of SIRT3 with UCP1, and ACSS1 with MUT and FFAR2, hinting at a less efficient thermogenic system. Recent findings show that adding propionate to mature adipocytes increases UCP1 and PGC1α, especially from mesenteric fat, enhancing mitochondrial respiration and ATP output (61)

In high-BAT individuals, ACSS2 expression also correlated with DNL genes like ACACA and ACLY, suggesting a coordinated balance between lipolysis and lipogenesis. Mice exposed to mild cold increase DNL gene expression via the AKT2-ChREBP pathway, which stimulates ACSS2 to convert acetate into acetyl-CoA for BAT utilisation (62). ACSS2 also recycles acetate from nuclear deacetylation reactions, such as HDAC activity (63–65) and can bind acetylated PPARγ, recruiting SIRT1 and PRDM16 to activate UCP1 transcription (65).

When comparing BAT and WAT depots, differences in the expression of ACSS1, ACSS2, and SIRT3 were observed only in the high-BAT group, suggesting a more metabolically flexible BAT capable of efficient substrate utilisation. Fatty acids not only fuel thermogenesis but also contribute to its activation in BAT (43,44,66). Interestingly, cold exposure simultaneously

induces β-oxidation and lipogenesis in BAT—two typically opposing pathways—highlighting BAT's unique metabolic coordination (44). In our study, high-BAT individuals displayed a more orchestrated metabolic profile linking SCFA signalling with lipolysis and lipogenesis, as observed from circulating SCFA associations and gene expression analysis. We also found correlations between SCFA pathway genes and AKT2 in high-BAT individuals and Elovl6 in both groups. AKT2 is a cold-inducible kinase that promotes ChREBP-mediated DNL, supplying fatty acids essential for mitochondrial heat production (62), whereas Elovl6 influences long-chain fatty acid composition, regulating mitochondrial efficiency and thermogenic adaptation. Elovl6 deficiency impairs lipid oxidation and cold response in BAT, emphasising its role in fuel management (66). These insights underscore the complexity of metabolic regulation in BAT and suggest that modulating lipid-derived signals and metabolic enzymes may offer therapeutic potential for metabolic disorders.

Our study does have limitations. Its cross-sectional design prevents causal inference, and differences between the two cohorts (such as in age and BMI) may have impacted BAT metabolic responses. While the sample size for gene expression analysis (n=14) is modest, it remains acceptable for human studies, and most blood markers and imaging data were collected from more individuals. The lack of dietary and microbiota data limits our conclusions on gut-derived SCFA production. Nonetheless, using two PET/CT radiotracers allowed a multidimensional assessment of BAT metabolism—including glucose and NEFA uptake, perfusion, and MRO_2—in relation to serum SCFAs. Although most of the genes are not exclusively involved in SCFA pathways, the integration of imaging data with serum SCFA levels and transcriptomic correlations suggests that these genes may act in concert to orchestrate SCFA handling and utilization within metabolically active BAT.

Our findings suggest that circulating SCFAs are not only markers but potential modulators of BAT function, especially under cold stress. During cold exposure, high-BAT individuals

maintained higher levels of circulating SCFAs while low-BAT individuals exhibited a drop in these metabolites. These differences were absent at room temperature, suggesting a specific SCFA resilience mechanism during thermal stress. Moreover, circulatory acetate levels correlated with BAT fatty acid uptake, and propionate with oxygen consumption, implying that stable SCFA levels support thermogenic substrate handling. These results support the hypothesis that maintaining SCFA availability—possibly through dietary fibre or microbiota-targeted interventions—may enhance BAT thermogenesis and systemic metabolic flexibility. Future clinical trials aimed at increasing endogenous SCFA production could help clarify the therapeutic potential of SCFA modulation in promoting BAT activity and metabolic health.

Data availability statement

The data that support the findings of this study are available from the corresponding author upon reasonable request and will be provided within a reasonable timeframe.

Funding information

The study was financially supported by Academy of Finland (grant numbers 259926, 265204, 269977, 272376, 292839, 314383, 314455, 314456, 321716, 335446, 335443, 335445, profi6 336449, 356733, 404030), the Finnish Cultural Foundation Southwest Finland Regional and Central Funds, the Turku University Hospital Research Funds, the Novo Nordisk Foundation (grant numbers NNF20OC0060547, NNF17OC0027232, NNF10OC1013354), the Finnish Diabetes Research Foundation, and European Commission (MSCA fellowship 101108436). T.F. and M.K. are funded by the German Research Foundation (BATenergy TRR333/1, Deutsche Forschungsgemeinschaft). The study was conducted within the Finnish Centre of Excellence in Cardiovascular and Metabolic Diseases, supported by the Academy of Finland, University of Turku, Turku University Hospital, and Abo Akademi University.

References

1. **Satija A, Hu FB.** Cardiovascular benefits of dietary fiber. *Curr Atheroscler Rep* 2012;14(6):505–514.

2. **Blaak EE, Canfora EE, Theis S, Frost G, Groen AK, Mithieux G, Nauta A, Scott K, Stahl B, van Harsselaar J, van Tol R, Vaughan EE, Verbeke K.** Short chain fatty acids in human gut and metabolic health. *Benef Microbes* 2020;11(5):411–455.

3. **Den Besten G, Van Eunen K, Groen AK, Venema K, Reijngoud DJ, Bakker BM.** The role of short-chain fatty acids in the interplay between diet, gut microbiota, and host energy metabolism. *J Lipid Res* 2013;54(9):2325–2340.

4. **Macfarlane S, Macfarlane GT.** Regulation of short-chain fatty acid production. *Proceedings of the Nutrition Society* 2003;62(1):67–72.

5. **Hu J, Lin S, Zheng B, Cheung PCK.** Short-chain fatty acids in control of energy metabolism. *Crit Rev Food Sci Nutr* 2018;58(8):1243–1249.

6. **Li D, Li Y, Yang S, Lu J, Jin X, Wu M.** Diet-gut microbiota-epigenetics in metabolic diseases: From mechanisms to therapeutics. *Biomedicine and Pharmacotherapy* 2022;153. doi:10.1016/j.biopha.2022.113290.

7. **Du Y, He C, An Y, Huang Y, Zhang H, Fu W, Wang M, Shan Z, Xie J, Yang Y, Zhao B.** The Role of Short Chain Fatty Acids in Inflammation and Body Health. *Int J Mol Sci* 2024;25(13). doi:10.3390/ijms25137379.

8. **Gao Z, Yin J, Zhang J, Ward RE, Martin RJ, Lefevre M, Cefalu WT, Ye J.** Butyrate improves insulin sensitivity and increases energy expenditure in mice. *Diabetes* 2009;58(7). doi:10.2337/db08-1637.

9. **Felix JB, Cox AR, Hartig SM.** Acetyl-CoA and Metabolite Fluxes Regulate White Adipose Tissue Expansion. *Trends in Endocrinology and Metabolism* 2021;32(5). doi:10.1016/j.tem.2021.02.008.

10. **Silva YP, Bernardi A, Frozza RL.** The Role of Short-Chain Fatty Acids From Gut Microbiota in Gut-Brain Communication. *Front Endocrinol (Lausanne)* 2020;11. doi:10.3389/fendo.2020.00025.

11. **O'Riordan KJ, Collins MK, Moloney GM, Knox EG, Aburto MR, Fülling C, Morley SJ, Clarke G, Schellekens H, Cryan JF.** Short chain fatty acids: Microbial metabolites for gut-brain axis signalling. *Mol Cell Endocrinol* 2022;546. doi:10.1016/j.mce.2022.111572.

12. **Canfora EE, Jocken JW, Blaak EE.** Short-chain fatty acids in control of body weight and insulin sensitivity. *Nat Rev Endocrinol* 2015;11(10). doi:10.1038/nrendo.2015.128.

13. **Forte N, Marfella B, Nicois A, Palomba L, Paris D, Motta A, Pina Mollica M, Marzo V Di, Cristino L.** The short-chain fatty acid acetate modulates orexin/hypocretin neurons: A novel mechanism in gut-brain axis regulation of energy homeostasis and feeding. *Biochem Pharmacol* 2024;226. doi:10.1016/j.bcp.2024.116383.

14. **Morrison DJ, Preston T.** Formation of short chain fatty acids by the gut microbiota and their impact on human metabolism. *Gut Microbes* 2016;7(3). doi:10.1080/19490976.2015.1134082.

15. **Li Z, Yi CX, Katiraei S, Kooijman S, Zhou E, Chung CK, Gao Y, Van Den Heuvel JK, Meijer OC, Berbée JFP, Heijink M, Giera M, Van Dijk KW, Groen AK, Rensen PCN, Wang Y.** Butyrate reduces appetite and activates brown adipose tissue via the gut-brain neural circuit. *Gut* 2018;67(7). doi:10.1136/gutjnl-2017-314050.

16. **Becher T, Palanisamy S, Kramer DJ, Eljalby M, Marx SJ, Wibmer AG, Butler SD, Jiang CS, Vaughan R, Schöder H, Mark A, Cohen P.** Brown adipose tissue is associated with cardiometabolic health. *Nat Med* 2021;27(1). doi:10.1038/s41591-020-1126-7.

17. **Herz CT, Kulterer OC, Prager M, Schmöltzer C, Langer FB, Prager G, Marculescu R, Kautzky-Willer A, Hacker M, Haug AR, Kiefer FW.** Active Brown Adipose Tissue Is Associated With a Healthier Metabolic Phenotype in Obesity. *Diabetes* 2022;71(1). doi:10.2337/db21-0475.

18. **Jurado-Fasoli L, Sanchez-Delgado G, Di X, Yang W, Kohler I, Villarroya F, Aguilera CM, Hankemeier T, Ruiz JR, Martinez-Tellez B.** Cold-induced changes in plasma signaling lipids are associated with a healthier cardiometabolic profile independently of brown adipose tissue. *Cell Rep Med* 2024;5(2). doi:10.1016/j.xcrm.2023.101387.

19. **Scheja L, Heeren J.** The endocrine function of adipose tissues in health and cardiometabolic disease. *Nat Rev Endocrinol* 2019;15(9). doi:10.1038/s41574-019-0230-6.

20. **Hu J, Kyrou I, Tan BK, Dimitriadis GK, Ramanjaneya M, Tripathi G, Patel V, James S, Kawan M, Chen J, Randeva HS.** Short-chain fatty acid acetate stimulates adipogenesis and mitochondrial biogenesis via GPR43 in brown adipocytes. *Endocrinology* 2016;157(5). doi:10.1210/en.2015-1944.

21. **Sahuri-Arisoylu M, Brody LP, Parkinson JR, Parkes H, Navaratnam N, Miller AD, Thomas EL, Frost G, Bell JD.** Reprogramming of hepatic fat accumulation and "browning" of adipose tissue by the short-chain fatty acid acetate. *Int J Obes* 2016;40(6). doi:10.1038/ijo.2016.23.

22. **Den Besten G, Bleeker A, Gerding A, Van Eunen K, Havinga R, Van Dijk TH, Oosterveer MH, Jonker JW, Groen AK, Reijngoud DJ, Bakker BM.** Short-chain fatty acids protect against high-fat diet-induced obesity via a pparg-dependent switch from lipogenesis to fat oxidation. *Diabetes* 2015;64(7). doi:10.2337/db14-1213.

23. **Wang D, Liu CD, Li HF, Tian ML, Pan JQ, Shu G, Jiang QY, Yin YL, Zhang L.** LSD1 mediates microbial metabolite butyrate-induced thermogenesis in brown and white adipose tissue. *Metabolism* 2020;102. doi:10.1016/j.metabol.2019.154011.

24. **He J, Zhang P, Shen L, Niu L, Tan Y, Chen L, Zhao Y, Bai L, Hao X, Li X, Zhang S, Zhu L.** Short-chain fatty acids and their association with signalling pathways in inflammation, glucose and lipid metabolism. *Int J Mol Sci* 2020;21(17). doi:10.3390/ijms21176356.

25. **Yamashita H, Maruta YH, Jozuka M, Kimura R, Iwabuchi H, Yamato M, Saito T, Fujisawa K, Takahashi Y, Kimoto M, Hiemori M, Tsuji H.** Effects of acetate on lipid metabolism in muscles

and adipose tissues of type 2 diabetic otsuka long-evans tokushima fatty (OLETF) Rats. *Biosci Biotechnol Biochem* 2009;73(3). doi:10.1271/bbb.80634.

26. **Orava J, Nuutila P, Noponen T, Parkkola R, Viljanen T, Enerbäck S, Rissanen A, Pietiläinen KH, Virtanen KA.** Blunted metabolic responses to cold and insulin stimulation in brown adipose tissue of obese humans. *Obesity* 2013;21(11). doi:10.1002/oby.20456.

27. **U Din M, Saari T, Raiko J, Kudomi N, Maurer SF, Lahesmaa M, Fromme T, Amri EZ, Klingenspor M, Solin O, Nuutila P, Virtanen KA.** Postprandial Oxidative Metabolism of Human Brown Fat Indicates Thermogenesis. *Cell Metab* 2018;28(2). doi:10.1016/j.cmet.2018.05.020.

28. **U-Din M, de Mello VD, Tuomainen M, Raiko J, Niemi T, Fromme T, Klåvus A, Gautier N, Haimilahti K, Lehtonen M, Kristiansen K, Newman JW, Pietiläinen KH, Pihlajamäki J, Amri EZ, Klingenspor M, Nuutila P, Pirinen E, Hanhineva K, Virtanen KA.** Cold-stimulated brown adipose tissue activation is related to changes in serum metabolites relevant to NAD+ metabolism in humans. *Cell Rep* 2023;42(9). doi:10.1016/j.celrep.2023.113131.

29. **Orava J, Nuutila P, Lidell ME, Oikonen V, Noponen T, Viljanen T, Scheinin M, Taittonen M, Niemi T, Enerbäck S, Virtanen KA.** Different metabolic responses of human brown adipose tissue to activation by cold and insulin. *Cell Metab* 2011;14(2). doi:10.1016/j.cmet.2011.06.012.

30. **Din MU, Raiko J, Saari T, Saunavaara V, Kudomi N, Solin O, Parkkola R, Nuutila P, Virtanen KA.** Human brown fat radiodensity indicates underlying tissue composition and systemic metabolic health. *Journal of Clinical Endocrinology and Metabolism* 2017;102(7). doi:10.1210/jc.2016-2698.

31. **Gjedde A.** Calculation of cerebral glucose phosphorylation from brain uptake of glucose analogs in vivo: A re-examination. *Brain Res Rev* 1982;4(2). doi:10.1016/0165-0173(82)90018-2.

32. **Patlak CS, Blasberg RG, Fenstermacher JD.** Graphical evaluation of blood-to-brain transfer constants from multiple-time uptake data. *Journal of Cerebral Blood Flow and Metabolism* 1983;3(1). doi:10.1038/jcbfm.1983.1.

33. **Chen KY, Cypess AM, Laughlin MR, Haft CR, Hu HH, Bredella MA, Enerbäck S, Kinahan PE, Lichtenbelt W van M, Lin FI, Sunderland JJ, Virtanen KA, Wahl RL.** Brown Adipose Reporting Criteria in Imaging STudies (BARCIST 1.0): Recommendations for Standardized FDG-PET/CT Experiments in Humans. *Cell Metab* 2016;24(2). doi:10.1016/j.cmet.2016.07.014.

34. **Fristedt R, Ruppert V, Trower T, Cooney J, Landberg R.** Quantitation of circulating short-chain fatty acids in small volume blood samples from animals and humans. *Talanta* 2024;272. doi:10.1016/j.talanta.2024.125743.

35. **Monfort-Pires M, U-Din M, de Mello V, Saari T, Raiko J, Kerminen E, Rajander J, Hanhineva K, Fromme T, Landberg R, Klingenspor M, Virtanen KA.** Supplementary file for Cold-induced serum short-chain fatty acids act as markers of brown adipose tissue metabolism in humans. 2025:1–4. https://figshare.com/articles/dataset/_b_Supplementary_file_for_b_b_Cold-induced_serum_short-chain_fatty_acids_act_as_markers_of_brown_adipose_tissue_metabolism_in_humans_b_/30383371?file=58827145

36. **Ichikawa N, Sasaki H, Lyu Y, Furuhashi S, Watabe A, Imamura M, Hayashi K, Shibata S.** Cold Exposure during the Active Phase Affects the Short-Chain Fatty Acid Production of Mice in a Time-Specific Manner. *Metabolites* 2022;12(1). doi:10.3390/metabo12010020.

37. **Lu Y, Fan C, Li P, Lu Y, Chang X, Qi K.** Short chain fatty acids prevent high-fat-diet-induced obesity in mice by regulating g protein-coupled receptors and gut Microbiota. *Sci Rep* 2016;6. doi:10.1038/srep37589.

38. **Moffett JR, Puthillathu N, Vengilote R, Jaworski DM, Namboodiri AM.** Acetate Revisited: A Key Biomolecule at the Nexus of Metabolism, Epigenetics and Oncogenesis—Part 1: Acetyl-CoA, Acetogenesis and Acyl-CoA Short-Chain Synthetases. *Front Physiol* 2020;11. doi:10.3389/fphys.2020.580167.

39. **Shi L, Tu BP.** Acetyl-CoA and the regulation of metabolism: Mechanisms and consequences. *Curr Opin Cell Biol* 2015;33. doi:10.1016/j.ceb.2015.02.003.

40. **Zou F, Qiu Y, Huang Y, Zou H, Cheng X, Niu Q, Luo A, Sun J.** Effects of short-chain fatty acids in inhibiting HDAC and activating p38 MAPK are critical for promoting B10 cell generation and function. *Cell Death Dis* 2021;12(6). doi:10.1038/s41419-021-03880-9.

41. **García-Carrizo F, Cannon B, Nedergaard J, Picó C, Dols A, Rodríguez AM, Palou A.** Regulation of thermogenic capacity in brown and white adipocytes by the prebiotic high-esterified pectin and its postbiotic acetate. *Int J Obes* 2020;44(3). doi:10.1038/s41366-019-0445-6.

42. **Sun W, Dong H, Wolfrum C.** Local acetate inhibits brown adipose tissue function. *Proc Natl Acad Sci U S A* 2021;118(49). doi:10.1073/pnas.2116125118.

43. **Bartelt A, Bruns OT, Reimer R, Hohenberg H, Ittrich H, Peldschus K, Kaul MG, Tromsdorf UI, Weller H, Waurisch C, Eychmüller A, Gordts PLSM, Rinninger F, Bruegelmann K, Freund B, Nielsen P, Merkel M, Heeren J.** Brown adipose tissue activity controls triglyceride clearance. *Nat Med* 2011;17(2). doi:10.1038/nm.2297.

44. **Wang Z, Wang QA, Liu Y, Jiang L.** Energy metabolism in brown adipose tissue. *FEBS Journal* 2021;288(12). doi:10.1111/febs.16015.

45. **Pedersen SS, Ingerslev LR, Olsen M, Prause M, Billestrup N.** Butyrate functions as a histone deacetylase inhibitor to protect pancreatic beta cells from IL-1β-induced dysfunction. *FEBS Journal* 2024;291(3). doi:10.1111/febs.17005.

46. **Kimura I, Inoue D, Maeda T, Hara T, Ichimura A, Miyauchi S, Kobayashi M, Hirasawa A, Tsujimoto G.** Short-chain fatty acids and ketones directly regulate sympathetic nervous system via G protein-coupled receptor 41 (GPR41). *Proc Natl Acad Sci U S A* 2011;108(19). doi:10.1073/pnas.1016088108.

47. **Yi W, Cheng J, Wei Q, Pan R, Song S, He Y, Tang C, Liu X, Zhou Y, Su H.** Effect of temperature stress on gut-brain axis in mice: Regulation of intestinal microbiome and central NLRP3 inflammasomes. *Science of the Total Environment* 2021;772. doi:10.1016/j.scitotenv.2020.144568.

48. **Li B, Li L, Li M, Lam SM, Wang G, Wu Y, Zhang H, Niu C, Zhang X, Liu X, Hambly C, Jin W, Shui G, Speakman JR.** Microbiota Depletion Impairs Thermogenesis of Brown Adipose Tissue and Browning of White Adipose Tissue. *Cell Rep* 2019;26(10). doi:10.1016/j.celrep.2019.02.015.

49. **Hernández MAG, Canfora EE, Jocken JWE, Blaak EE.** The short-chain fatty acid acetate in body weight control and insulin sensitivity. *Nutrients* 2019;11(8). doi:10.3390/nu11081943.

50. **Müller M, Hernández MAG, Goossens GH, Reijnders D, Holst JJ, Jocken JWE, van Eijk H, Canfora EE, Blaak EE.** Circulating but not faecal short-chain fatty acids are related to insulin sensitivity, lipolysis and GLP-1 concentrations in humans. *Sci Rep* 2019;9(1). doi:10.1038/s41598-019-48775-0.

51. **Al-Lahham S, Roelofsen H, Rezaee F, Weening D, Hoek A, Vonk R, Venema K.** Propionic acid affects immune status and metabolism in adipose tissue from overweight subjects. *Eur J Clin Invest* 2012;42(4). doi:10.1111/j.1365-2362.2011.02590.x.

52. **Comerford SA, Huang Z, Du X, Wang Y, Cai L, Witkiewicz AK, Walters H, Tantawy MN, Fu A, Manning HC, Horton JD, Hammer RE, Mcknight SL, Tu BP.** Acetate dependence of tumors. *Cell* 2014;159(7). doi:10.1016/j.cell.2014.11.020.

53. **Shi T, Wang F, Stieren E, Tong Q.** SIRT3, a mitochondrial sirtuin deacetylase, regulates mitochondrial function and thermogenesis in brown adipocytes. *Journal of Biological Chemistry* 2005;280(14). doi:10.1074/jbc.M414670200.

54. **Ansari A, Rahman MS, Saha SK, Saikot FK, Deep A, Kim KH.** Function of the SIRT3 mitochondrial deacetylase in cellular physiology, cancer, and neurodegenerative disease. *Aging Cell* 2017;16(1):4–16.

55. **Sakakibara I, Fujino T, Ishii M, Tanaka T, Shimosawa T, Miura S, Zhang W, Tokutake Y, Yamamoto J, Awano M, Iwasaki S, Motoike T, Okamura M, Inagaki T, Kita K, Ezaki O, Naito M, Kuwaki T, Chohnan S, Yamamoto TT, Hammer RE, Kodama T, Yanagisawa M, Sakai J.** Fasting-Induced Hypothermia and Reduced Energy Production in Mice Lacking Acetyl-CoA Synthetase 2. *Cell Metab* 2009;9(2). doi:10.1016/j.cmet.2008.12.008.

56. **Sebaa R, Johnson J, Pileggi C, Norgren M, Xuan J, Sai Y, Tong Q, Krystkowiak I, Bondy-Chorney E, Davey NE, Krogan N, Downey M, Harper ME.** SIRT3 controls brown fat thermogenesis by deacetylation regulation of pathways upstream of UCP1. *Mol Metab* 2019;25. doi:10.1016/j.molmet.2019.04.008.

57. **Giralt A, Villarroya F.** SIRT3, a pivotal actor in mitochondrial functions: Metabolism, cell death and aging. *Biochemical Journal* 2012;444(1). doi:10.1042/BJ20120030.

58. **Jash S, Banerjee S, Lee MJ, Farmer SR, Puri V.** CIDEA Transcriptionally Regulates UCP1 for Britening and Thermogenesis in Human Fat Cells. *iScience* 2019;20. doi:10.1016/j.isci.2019.09.011.

59. **Barneda D, Planas-Iglesias J, Gaspar ML, Mohammadyani D, Prasannan S, Dormann D, Han GS, Jesch SA, Carman GM, Kagan V, Parker MG, Ktistakis NT, Klein-Seetharaman J, Dixon AM, Henry SA, Christian M.** The brown adipocyte protein CIDEA promotes lipid droplet fusion via a

phosphatidic acid-binding amphipathic helix. *Elife* 2015;4(NOVEMBER2015). doi:10.7554/eLife.07485.

60. **Hirschey MD, Shimazu T, Goetzman E, Jing E, Schwer B, Lombard DB, Grueter CA, Harris C, Biddinger S, Ilkayeva OR, Stevens RD, Li Y, Saha AK, Ruderman NB, Bain JR, Newgard CB, Farese R V., Alt FW, Kahn CR, Verdin E.** SIRT3 regulates mitochondrial fatty-acid oxidation by reversible enzyme deacetylation. *Nature* 2010;464(7285). doi:10.1038/nature08778.

61. **Lu B, Hanyaloglu AC, Ma Y, Frampton AE, Limb C, Merali N, Pai M, Ahmed R, Christian M, Frost G.** Propionate Induces Energy Expenditure via Browning in Mesenteric Adipose Tissue. *J Clin Endocrinol Metab* 2025. doi:10.1210/clinem/dgaf280.

62. **Sanchez-Gurmaches J, Tang Y, Jespersen NZ, Wallace M, Martinez Calejman C, Gujja S, Li H, Edwards YJK, Wolfrum C, Metallo CM, Nielsen S, Scheele C, Guertin DA.** Brown Fat AKT2 Is a Cold-Induced Kinase that Stimulates ChREBP-Mediated De Novo Lipogenesis to Optimize Fuel Storage and Thermogenesis. *Cell Metab* 2018;27(1). doi:10.1016/j.cmet.2017.10.008.

63. **Huang Z, Zhang M, Plec AA, Estill SJ, Cai L, Repa JJ, McKnight SL, Tu BP.** ACSS2 promotes systemic fat storage and utilization through selective regulation of genes involved in lipid metabolism. *Proc Natl Acad Sci U S A* 2018;115(40). doi:10.1073/pnas.1806635115.

64. **Bulusu V, Tumanov S, Michalopoulou E, van den Broek NJ, MacKay G, Nixon C, Dhayade S, Schug ZT, Vande Voorde J, Blyth K, Gottlieb E, Vazquez A, Kamphorst JJ.** Acetate Recapturing by Nuclear Acetyl-CoA Synthetase 2 Prevents Loss of Histone Acetylation during Oxygen and Serum Limitation. *Cell Rep* 2017;18(3). doi:10.1016/j.celrep.2016.12.055.

65. **Chen N, Zhao M, Wu N, Guo Y, Cao B, Zhan B, Li Y, Zhou T, Zhu F, Guo C, Shi Y, Wang Q, Li Y, Zhang L.** ACSS2 controls PPARγ activity homeostasis to potentiate adipose-tissue plasticity. *Cell Death Differ* 2024;31(4). doi:10.1038/s41418-024-01262-0.

66. **Tan CYY, Virtue S, Bidault G, Dale M, Hagen R, Griffin JLL, Vidal-Puig A.** Brown Adipose Tissue Thermogenic Capacity Is Regulated by Elovl6. *Cell Rep* 2015;13(10). doi:10.1016/j.celrep.2015.11.004.

Figure legends

Figure 1. Correlations between NEFA uptake (A), metabolic rate of oxygen (B), and glucose uptake rate in cold-stimulated BAT (C) with cold circulating acetate, and propionate (D, E, F respectively), and circulating acetate (G), propionate (H), and butyrate (I), at room temperature (RT) and after 2 hours of cold exposure (Cold) (log-transformed data). Sample sizes differed for different tracers. Cold-stimulated NEFA uptake (A and D; n=35); metabolic rate of oxygen (B and E; n = 19), and glucose uptake rate (C and F; n=35). For the comparisons between RT and CI-SCFA (Panels G-I) n = 33.

Figure 2. Circulating acetate (A), propionate (B), and butyrate (C) at room temperature and after 2 hours of cold exposure in low- versus high-BAT volunteers and Spearman's correlations between circulating room temperature (D, E) and cold-induced (F, G) SCFA with clinical variables. Bigger circles indicate stronger correlation analysis or lower p-values. Circulating SCFA (RT: n = 33, CI: n = 72). RT-BAT NEFA uptake (n = 18), RT-BAT glucose uptake (n = 18), RT-BAT perfusion (n = 25), RT-BAT MRO2 (n = 6), CI-BAT NEFA uptake (n = 35), CI-BAT glucose uptake (n = 35), CI-BAT perfusion (n = 54), CI-BAT MRO2 (n = 19).

Figure 3. Heat map of correlations between BAT markers with genes from SCFA pathway and *de novo* lipogenesis genes according to low- (panel A, n = 5) and high-BAT (panel B, n = 9) and heat map with split tiles (Low-bAT versus high-BAT, panel C) and differences in gene expression in WAT and BAT according to the same groups (D-K).

Figure 4. Proposed mechanism linking SCFA metabolism to BAT function.

Cold exposure modulates SCFAs—acetate, butyrate, and propionate—which support BAT thermogenesis. In high-BAT individuals, SCFAs are preserved during cold and correlate with NEFA uptake. Upon entering brown adipocytes, acetate is converted by ACSS2 to acetyl-CoA,

fueling lipogenesis (via *ACC, FASN, SCD1*) and histone acetylation, which promotes thermogenic gene expression (*PGC-1α*). Fatty acids are mobilised (HSL) and imported via *CD36, FABP4, and FATP*. Butyrate enhances mitochondrial biogenesis and browning by inhibiting HDACs and increasing acetyl-CoA via ACSS1. Propionate is metabolised to succinyl-CoA (via *ACSS3, PCCA, PCCB, and MUT*), enters the TCA cycle, and activates *SIRT3* to boost NAD^+ and ETC activity. Cold and β-adrenergic signalling (NE, β-AR) further promote SCFA uptake and acetate production. Genes involved in SCFA catabolism are enriched in BAT and associate with thermogenesis (*UCP1, PRDM16*), β-oxidation (*HADHA/B, ECHS1*), and lipogenesis (*FASN, ACLY*), linking SCFA availability to metabolic and epigenetic control of browning. Abbreviations: ACSS1/2/3 – acyl-CoA synthetase short-chain family members 1–3; ACC – acetyl-CoA carboxylase; FASN – fatty acid synthase; SCD1 – stearoyl-CoA desaturase 1; HSL – hormone-sensitive lipase; CD36, FABP4, FATP – fatty acid transporters; PGC-1α – peroxisome proliferator-activated receptor gamma coactivator 1-alpha; UCP-1: uncoupling protein 1; PCCA/PCCB – propionyl-CoA carboxylase subunits; MUT – methylmalonyl-CoA mutase; SIRT3- sirtuin 3; ETC – electron transport chain; TCA – tricarboxylic acid cycle; TAG – triacylglycerol; FA – fatty acid; DNL – de novo lipogenesis; HDAC – histone deacetylase; NE – norepinephrine; β-AR – beta-adrenergic receptor; FFAR2/3 – free fatty acid receptors 2 and 3 (Created in BioRender. Pires, M. (2025) https://BioRender.com/js8rqie).

Table 1. Clinical data and circulating short-chain fatty acids in low-BAT and high-BAT individuals.

	Low-BAT (n=32)	High-BAT (n=39)	p-value	Total sample
Clinical data				
Female participants (n; %)	17 (53%)	32 (82%)	<0.01	49
Age (years)#	43.7 ± 7.5	35.9 ± 10.7	<0.01	39.4 ± 10.1
Weight (kg)	88.7 ± 19.1	70.6 ± 12.4	<0.01	78.7 ± 18.1
BMI (kg/m^2)	29.8 ± 6.5	24.8 ± 3.8	<0.01	27.1 ± 5.7
Body Fat (%)	33.5 ± 11.3	31.8 ± 8.1	0.46	32.5 ± 9.6
Waist circumference (cm)	98.2 ± 18.7	84.2 ± 12.9	<0.01	90.7 ± 17.2
Hips circumference (cm)#	106.6 ± 14.3	97.9 ± 9.8	<0.01	101.9 ± 12.8
Insulin sensitivity (M-value) (µmol/kg/min)	30.3 ± 17.7	47.1 ± 20.2	<0.01	39.8 ± 20.8
HDL-c (mmol/L)	1.5 ± 0.3	1.7 ± 0.4	0.04	1.6 ± 0.4
Total cholesterol (mmol/L)	5.0 ± 0.8	4.4 ± 0.9	<0.01	4.7 ± 0.9
LDL-c (mmol/L)#	3.0 ± 0.8	2.5 ± 0.7	<0.01	2.7 ± 0.8
Triglycerides (mmol/L)#	1.2 ± 0.7	0.8 ± 0.3	<0.01	1.0 ±0.5
Serum SCFA (RT) (n = 33)				
Fasting acetate (µM)#	103.2 ± 63.0	125.6 ± 75.5	0.47	124.7 ± 84.0
Fasting propionate (µM)#	1.4 ± 0.6	1.5 ± 0.8	0.78	1.4 ± 0.7
Fasting butyrate (µM)#	0.4 ± 0.3	0.4 ± 0.17	0.37	0.4 ± 0.2
Serum SCFA (cold stimulation – CI) (n = 72)				
Fasting acetate (µM)#	91.1 ± 50.7	121.3 ± 80.0	0.06	106.0 ± 69.3

Fasting propionate (μM)	0.9 ± 0.5	1.2 ± 0.6	0.02	1.1 ± 0.5
Fasting butyrate (μM)[#]	0.2 ± 0.1	0.4 ± 0.4	0.13	0.3 ± 0.3
BAT-imaging data (Room temperature)				
Glucose uptake rate (μmol/100 g/min)	1.0 ± 0.2	1.0 ± 0.6	0.48	1.0 ± 0.4
NEFA uptake rate (μmol/100 g/min)	0.3 ± 0.2	0.9 ± 0.7	<0.01	0.6 ± 0.6
Perfusion (mL/100g/min)	4.9 ± 3.7	8.1 ± 4.0	0.02	6.7 ± 4.1
Metabolic rate of oxygen (MRO_2) (mL/100g/min)	0.5 ± 0.1	0.7 ± 0.1	0.13	0.6 ± 0.1
BAT-imaging data (after Cold-stimulation - CI)				
Glucose uptake rate (μmol/100 g/min)	1.1 ± 0.6	8.1 ± 5.5	<0.01	4.9 ± 5.3
NEFA uptake (μmol/100 g/min)	0.4 ± 0.1	1.4 ± 1.1	<0.01	1.0 ± 0.9
Perfusion (mL/100g/min)	9.8 ± 4.0	14.8 ± 6.6	<0.01	12.9 ± 6.2
Metabolic rate of oxygen (MRO_2)	1.3 ± 0.4	1.8 ± 0.6	0.076	1.6 ± 0.6

1 Independent-samples t-test/[#]non-parametric test (Mann-Whitney U)

2

3

4

5

6

7

8

9

10

Figure 1.

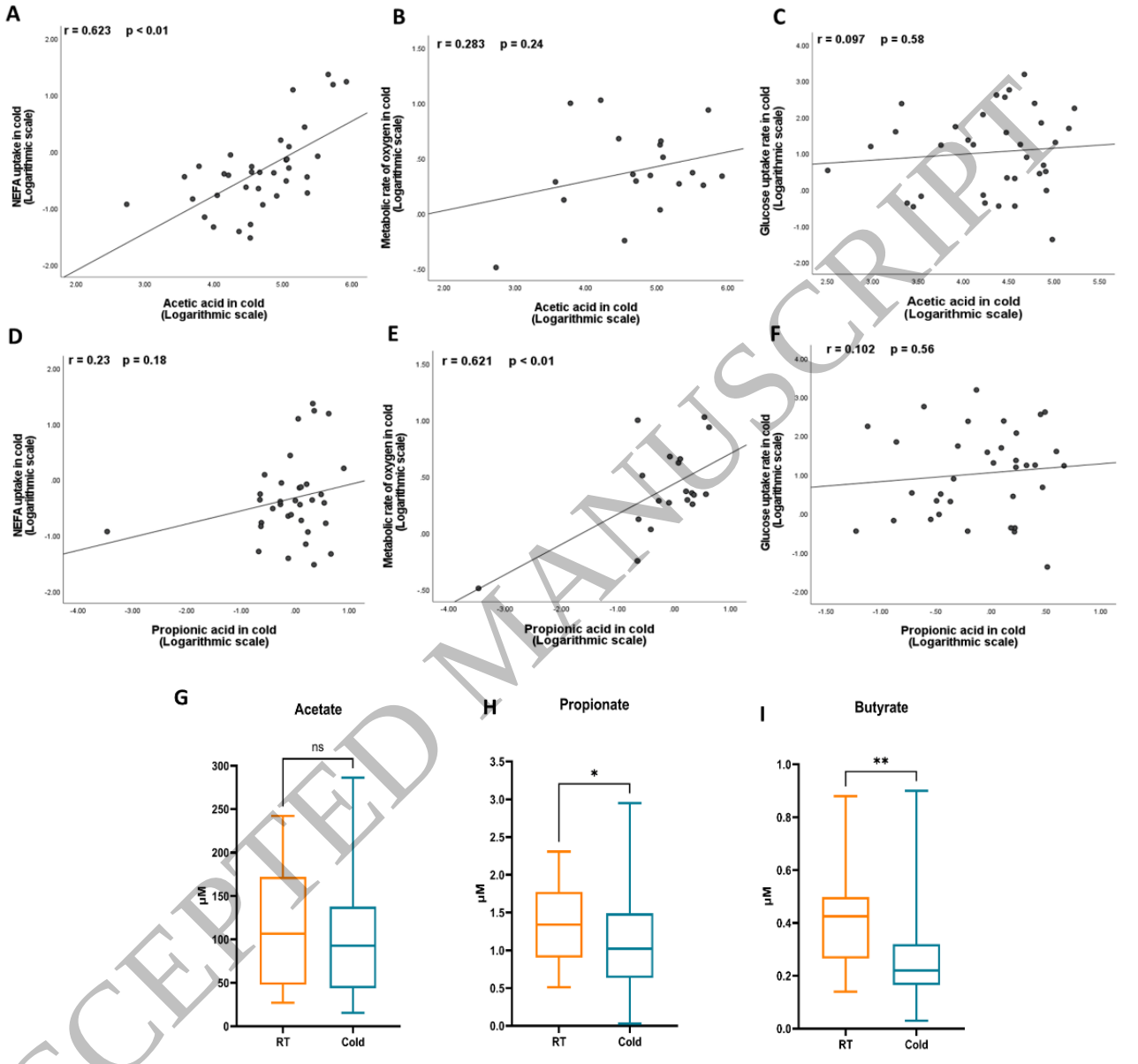

Ns: non significant/*p<0.05/**p<0.01/***p<0.001/****p<0.0001

Figure 2.

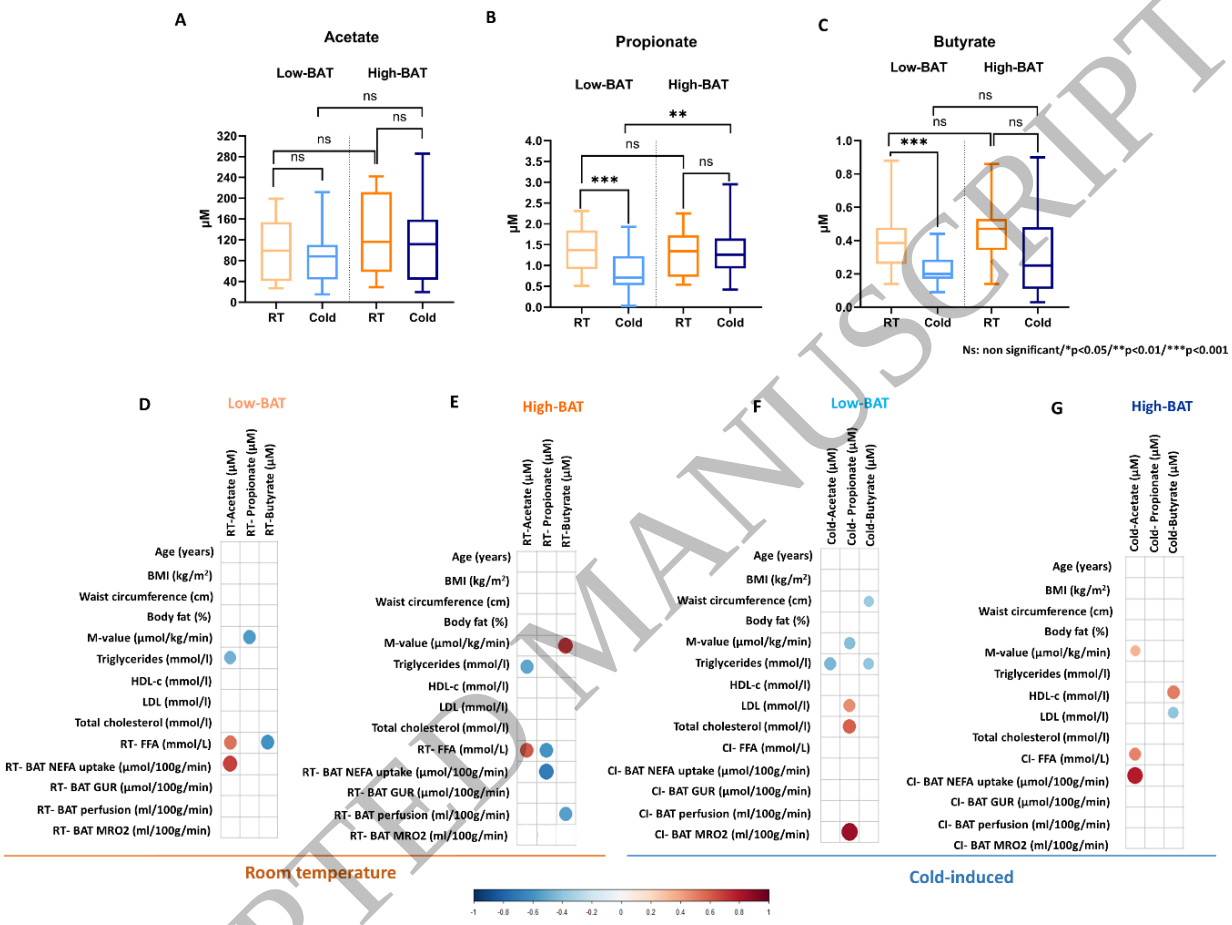

Figure 3.

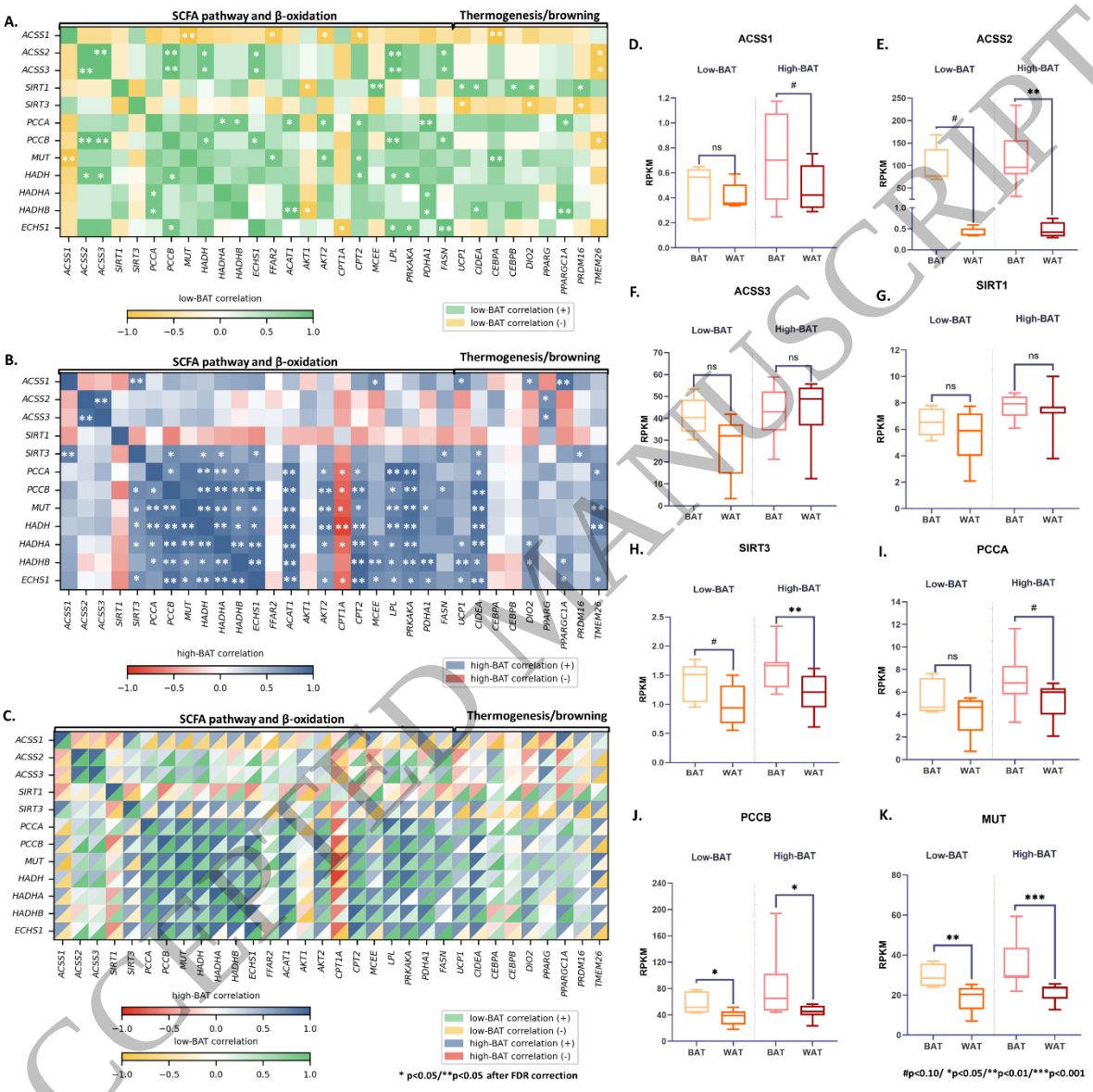

Figure 4.